DOI: 10.2478/cipms-2021-0005 Curr. Issues Pharm. Med. Sci., Vol. 34, No. 1, Pages 20-27

Current Issues in Pharmacy and Medical Sciences
Formerly ANNALES UNIVERSITATIS MARIAE CURIE-SKLODOWSKA, SECTIO DDD, PHARMACIA

journal homepage: http://www.curipms.umlub.pl/

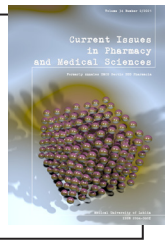

Molecular docking study of the acetylcholinesterase inhibition

Amina Merzoug[1,2*], Hanane Boucherit[1,2], Rima Khaled[2], Amel Chefiri[2], Abdelouahab Chikhi[1], Abderrahmane Benseguени[1]

[1] Laboratory of Applied Biochemistry, Department of Biochemistry and Cellular and Molecular Biology, Faculty of Natural and Life Sciences, Mentouri Brothers University, Algeria
[2] Abdelhafid Boussouf University Center, Mila, Algeria

ARTICLE INFO

Received 12 November 2020
Accepted 02 January 2021

Keywords:
acetylcholinesterase,
Alzheimer's disease,
FlexX,
molecular docking,
ZINC database.

ABSTRACT

While Alzheimer disease is the most common form of dementia, acetylcholinesterase is an interesting therapeutic target for the development of new anti-Alzheimer's disease drugs. In order to discover potential compounds inhibiting this protein target, a molecular docking study of a similar collection of 1-[[2,4-bis[(E)hydroxyiminomethyl] pyridin-1-ium-1-yl]methoxymethyl] pyridin-1-ium-4-carboxamide (HLO) inhibitor from ZINC database using FlexX program was realized. Before performing the molecular docking, FlexX was validated by Root mean square deviation test to determine the reproducibility of the docking program. The strategy undertaken in this study permitted us to propose products 4-[[2-[(Z)-N'-hydroxycarbamimidoyl]-4-pyridyl]methylamino] benzamide and N-[(E)-[1-(4-nitrophenyl)pyrrol-2-yl]methylene amino]isonicotinamide as potential new inhibitors of humane acetylcholinesterase. The two proposed products may act as strong anti-Alzheimer leads compounds.

INTRODUCTION

Alzheimer's disease is a chronic neurodegenerative pathology, accounting for 60-70% of all cases of dementia and touching about 6% of all persons 65 years and older [1,2]. Many studies relate the deteriorated cognitive functions of Alzeheimer patients with the reduced synthesis of the neurotransmitter acetylcholine that is released into the synapses of the nervous system [3-5]. Acetylcholinesterase (AChE; EC 3.1.1.7) is a critical enzyme that regulates neurotransmission by catalyzing the degradation of the acetylcholine [6]. The capacity of this enzyme increases in Alzheimer's patients, which make it a target of interest in the search of new treatment [7].

Four anti-AChE agents are currently used as Alzheimer's disease drugs. These are tacrine, rivastigmine, donepezil and galantamine [8]. However, the application of these drugs is limited by their severe side effects, including hepatotoxic liability [9], muscle cramps [10] diarrhea and vomiting [11,12]. Therefore, it is still necessary to develop new products to treat Alzheimer's disease. Structural studies of the AChE active site show that it has two adjacent pockets to which ligands may bind - the peripheral pocket at the entrance of the cavity and the catalytic pocket at its bottom [13-16]. In the catalytic pocket, the Ser203, His447 and Glu334 are the key residues for the substrate hydrolyzation [13]. Tyr72, Tyr124 and Trp286 amino acids play an essential role in the interaction between the ligand and the peripheral pocket.

The object of the present work was to analyze the interactions involved in the inhibition of AChE by various compounds listed in the Protein Data Bank (PDB) and in a collection of derivatives of the inhibitor that had the greatest affinity, by means of applying the molecular docking method. This is one of the commonly used computational strategies in structure-based drug design [17]. The intent is to realize a computational absorption, distribution, metabolism, excretion and toxicity (ADME/Tox) prediction for exploring the best possible inhibitors for AChE. These actions may aid the development of more efficient anti-Alzheimer's disease agents.

MATERIALS AND METHOD

Protein preparation

The enzyme selected as a pharmacological target for the work was acetylcholinesterase, the 3D structure of which was retrieved from the PDB (PDB ID: 4M0E) [18]. It has two identical chains (A, B). In the protein structure preparation, chain B was removed and the co-crystal selective inhibitor 1YL was used for active site determination. The

* **Corresponding author**
e-mail: a.merzouk@centre-univ-mila.dz

residues Tyr72, Asp74, Gly121, Tyr124, Trp286, His287, Leu289, Gln291, Glu292, Ser293, Val294, Phe295, Arg296, Phe297, Tyr337, Phe338, Tyr341, Gly342 His447 and four water molecules were found to be present in the binding pocket of the proposed target enzyme.

Molecular docking

In order to assess by means of the molecular docking approach, the interaction modes and orientation on the AChE binding pocket of 82 inhibitors listed in the PDB and in a collection of 119 derivatives of the inhibitors that had the greatest affinity to the binding site, we used the most recent version of FlexX software (2.3.3, 2017).

The three-dimensional structures of the derivative compounds were downloaded in the sdf. format from the ZINC database (http://zinc.docking.org), a commercially available library of 35 million chemical products with vendors and product proprieties information.

ADME/Tox

To predict the pharmacokinetic properties of the most promising products presaged by molecular docking, a computational ADME/Tox study was performed using Swissadme (http://www.swissadme.ch) for blood-brain barrier (BBB) penetration, gastrointestinal absorption (GI), and Cytochrome P450 (CYP) inhibition. Moreover, PreADMET (https://preadmet.bmdrc.kr) was employed to establish cell permeability (COCA-2) and toxicity.

All potential drugs had to met Lipinski's Rule of Five, which states that likely orally active drug must complete two of these four proprieties [19]:

- no more than 5 hydrogen bond donors;
- no more than 10 hydrogen bond acceptors;
- the molecular weight under 500 g/mol^{-1};
- the Log P below 5.

RESULTS AND DISCUSSION

Ability of docking protocol

Before performing the molecular docking study, the docking protocol was validated. The co-crystal selective ligands were, therefore, removed from 240 crystallized protein-ligand complexes listed in the PDB (Tab. 1) and again docked back into the binding site of the proteins. Root mean square deviation (RMSD) of 78.55% of the ligands in co-crystal complex conformations and the best-docked conformations were less than 2Å. Most ligands showed deviations that were negligible (Fig. 1). This indicated the capacity of the docking protocol to reproduce the interaction modes and orientations of the co-crystal ligands [20].

Study of the interactions involved in the inhibition of AChE by various compounds

With the aim of identifying new inhibitors of AChE, we studied firstly the mechanism of inhibition set up by 82 known inhibitors itemized in the PDB. The results of the simulation by FlexX of these inhibitors are represented below in Table 2.

The results presented in Table 2 reveal that among the 82 docked inhibitors, compound 1-[[2,4-bis[(E) hydroxyiminomethyl] pyridin-1-ium-1-yl]methoxymethyl] pyridin-1-ium-4-carboxamide (HLO) demonstrated the highest score, and hence, is the most potent inhibitor of AchE. For this reason, we have chosen this compound as reference model to interpret the diverse established links with the protein in question, and as starting structure for the development of new potent inhibitors.

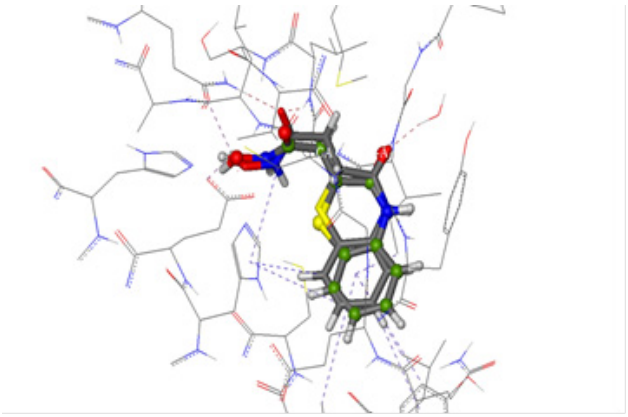

Figure 1. Overlay of co-crystal ligand NLP conformation extracted from 2GU4 (colored in grey) with the best-docked conformation (colored in green)

The presented docking study reveals that the compound HLO fits favorably into the AChE binding pocket as it displays hydrogen bonds with Trp286, Leu289, Ser293, Tyr337 (Fig. 2), as well as hydrophobic interactions with Tyr72, Tyr124, Trp286, His287, Leu289, Tyr341 (Fig. 3) with a binding energy of -34,4450 kj/mol.

Accordingly:

- A hydrogen bridge is observed between the carbonyl of the inhibitor and the water molecule H2O 901 present in the binding pocket (O1……H- H2O 901);
- Two hydrogen bridges are observed between the amine function of the inhibitor and the two carbonyl groups of Trp286 (N3-H……O-Trp286) and Leu289 (N3-H……O-Leu289);
- Two hydrogen bonds are observed between the nitrogen atoms of the inhibitor and the water molecules H2O 715 (N16……H- H2O 715) and H2O 857 (N23…… H- H2O 857) presents in the binding site;
- Two hydrogen bridges are established between the hydroxyl group of the inhibitor and the carbonyl function of Ser293 (H-O17……O-Ser293) on the one hand and the hydroxyl function of Tyr337 on the other hand (H-O14……O-Tyr337).

The ZINC database was used to find the structural analogues of the inhibitor HLO in order to dock them by FlexX on the human AChE crystallographic structure, 4M0E, and to search among them for those that bind more strongly than the HLO to our target AChE. We then compared the binding energies of these compounds (Tab. 3) with the reference inhibitor, HLO, and proposed the best inhibitors of the enzyme in question.

Of the 119 inhibitors tested, the compounds 4-[[2-[(Z)-N'-hydroxycarbamimidoyl]-4-pyridyl]methylamino] benzamide (ZINC78954474) and N-[(E)-[1-(4-nitrophenyl)pyrrol-2-yl]methylene amino]isonicotinamide (ZINC00123616) showed lower binding energies than the reference inhibitor (Tab. 3). They also formed the most stable AChE-inhibitor

complexes. Hence, we propose that these two compounds can interact efficiently with the enzyme. Further work was then undertaken to elucidate the mechanism of interaction of these proposed compounds.

Table 1. List of 240 complexes used to test the ability of the docking protocol

Enzyme code	Inhibitor code	RMSD (Å)	Enzyme code	Inhibitor code	RMSD (Å)	Enzyme code	Inhibitor code	RMSD (Å)
4M0E	1YL	0.9502	2HA3	CHT	2.5355	2XUQ	TZ4	1.3917
5FOG	GCB	0.7738	2J3Q	TFL	0.6751	3DL4	P6G	5.9637
1AX9	EDR	0.5188	2JEY	HLO	1.0675	3ZLT	PGO	2.9450
2ACK	EDR	0.3768	2JFO	HBP	2.0238	3ZLV	HI6	0.3776
2WHR	K27	0.3881	2VQ6	FP1	1.2423	4A23	C56	0.4103
3M3D	PG4	1.3365	2WLS	X13	0.8930	4ARA	C56	1.0888
1DX6	GNT	0.5148	6CQW	HI6	0.8212	4ARB	C57	0.7511
1E66	HUX	0.5944	6CQU	HI6	4.3540	4B7Z	PEG	1.5925
1GPN	HUB	0.6544	6CQV	HI6	2.8438	4B8O	PEG	1.7046
2C58	ETM	0.6814	6EZH	C6H	1.7114	4B81	PEG	2.0632
2JEZ	HLO	0.7767	6EZG	C6H	2.5989	4B82	B3Z	1.6736
3ZLU	1KA	1.5215	5OV9	PE4	2.7692	4B83	B3V	1.1221
6EWK	RMO	0.5662	1N5M	GMN	1.5301	4B84	Z5K	2.0024
2XUD	DME	1.3136	1J07	DCU	2.2569	4B85	B3W	1.4123
1ACL	DME	1.7168	1J06	AE3	2.9054	4BCO	SO4	0.7938
1ACJ	THA	0.5243	3DL7	P6G	0.9210	4BDT	HUW	0.5076
5E4J	DME	1.5373	2JGK	P6G	2.6636	4EY5	HUP	0.3100
5DLP	SO4	0.9518	2JGJ	AE3	2.8217	5HF5	EDO	0.5691
5EIE	ACT	0.4865	2JGF	P6G	4.1626	5HF6	EDO	0.5898
1Q84	TZ4	0.5954	2JGL	P6G	2.7171	5HF8	EDO	0.8023
3ZV7	PEG	0.6458	2JGI	AE3	5.0399	5HF9	HI6	1.3671
1N5R	1CY	0.8627	6CQZ	VX	1.5635	5HFA	FP1	0.7177
2X8B	SO4	0.6766	6CQX	7PE	2.5366	4EY7	GNT	0.3916
5EIH	ACT	0.4289	5HQ3	MES	1.5038	4EY8	E20	0.7238
5EHQ	5O2	1.0668	5E2I	PEG	1.4563	4TVK	SO4	0.3913
1GQS	SAF	0.6484	5EIE	PG4	2.6792	4W63	TJH	1.0833
1VOT	HUP	0.4708	5EIA	PG4	4.7369	4X3C	HIB	3.9986
2C4H	PGE	1.4454	5EHZ	5NZ	1.6242	5BWB	TNH	3.6490
2C5G	ETM	0.6527	5EHN	P6G	3.0123	5BWC	4VV	1.8078
2HA0	P6G	1.5995	2HA2	SCK	1.1327	5DTJ	HBP	0.9884
2XU0	TZ4	2.5338	2HA5	ACT	0.3527	5E4T	5GB	2.4733
2XUP	TZ5	1.2976	2XI4	AFT	0.5179	5EHX	MBT	0.7210
2XUQ	TZ4	1.3917	5FPP	HI6	0.6425	5EI5	AE4	3.1581
4EY6	AA7	3.0474	1C24	PFU	6.6307	3TT2	O7N	0.5873
4U73	Q02	0.4094	2GG2	M12	1.1639	4EM7	ORA	0.7011
5LYX	7BF	1.9080	2GG3	M13	1.1867	4EMV	OR9	0.4311
5IB9	BES	0.6464	2GGB	U17	0.9611	4LPO	1YM	0.6500
4XND	HT7	0.7431	2OAZ	196	1.3077	4LPB	1YP	0.6344
3Q7J	FBO	1.6734	2P99	2P9A	0.4150	5BOC	TSJ	2.4491
1G27	BB1	0.9022	3IU7	1XNZ	0.5235	5BS8	MFX	3.6761
4EOX	OS5	1.1344	2ADU	2ADU	0.5179	5BTA	MFX	1.2867
2AI8	SB7	0.9193	2BB7	QMS	0.1594	5BTC	CPF	1.5176
3M6Q	BB2	0.9429	2GU4	NLP	0.0283	5BTD	GNF	4.1934
3M6R	BB2	1.0015	2GU5	NLP	1.1581	5BTF	GNF	7.7439
3O3J	BB4	0.6533	2GU6	NLP	0.6433	5BTG	LFX	3.3794
3U7K	MDB	0.6623	2Q92	B23	0.6552	5BTI	LFX	4.8256
3U7M	FHF	4.0437	2Q93	B21	0.4706	5BTL	8MX	3.2485
3U7N	UHF	2.0083	2Q94	A04	0.4430	3QX3	EVP	5.1885
5CWY	4WL	0.4652	2Q95	A05	0.7386	4GO4	ASN	1.5770

5CY7	56U	0.6061	2Q96	A18	0.5771	4GOV	MIX	6.1906
5CY8	56V	0.4530	4IF7	HCM	0.7846	465D	9AD	0.7673
5MTE	BB2	0.8852	4Z7M	427M	1.5471	1CYO	A3P	5.9194
5JF1	BB2	0.9775	1C27	NLP	0.8954	1CY7	PO4	1.2626
5JF6	BB4	0.7885	2EVC	FC3	0.5437	3FOC	NFX	4.8770
5JF8	PN3	0.5193	2G6P	HM2	1.0061	3FV5	1EU	0.5342
3PN3	BN3	3.1723	4FLL	YZ6	1.1956	4Z4Q	PDQ	2.7545
3PN4	BD2	0.8548	EVO	CTO	1.4476	1L8I	EHD	3.5061
2AIA	SB8	1.5430	2EVM	FC2	0.3260	1T8I	TTJ	3.5061
5VCP	BB2	0.8185	3PKB	Y16	0.7731	5BOD	RXV	0.9883
1G2A	BB2	0.7577	3PKC	Y08	1.1691	2XCS	RXV	3.9899
1S17	GNR	0.3008	4FLJ	Y08	1.1691	5L 3J	6G9	0.9875
1WS1	BB2	0.9348	1R5G	A01	1.4255	2XCT	CPF	2.9560
2EW5	Y12	1.3292	1R5H	A02	0.9170	4K40	DOO	1.2477
2EW6	Y13	0.9684	4CPM	G39	0.4185	3CL0	G39	0.3994
2KMN	BB2	1.4302	4GZP	G39	0.6194	2HT7	G39	0.5128
1LQY	BB2	0.6687	4HZZ	G39	0.3319	6EKU	ZMR	0.6360
1LRU	BB2	0.8999	5B2D	SLT	3.2417	1IVD	ST1	0.8785
3G5K	BB2	0.7379	5KKY	6VD	0.6277	3K37	BCZ	0.3368
3K6I	2BB	0.4604	1A4Q	DPC	0.8848	4HZW	LNV	0.4672
3M6P	BB2	0.8042	1B9T	RAI	0.8268	4HZX	G39	0.3692
4DR9	BB2	1.0375	1B9V	RA2	0.6461	4MJU	27S	0.7077
4U73	Q02	0.4094	2QWD	4AM	0.5061	4MJV	27V	1.2499
1I7H	BCZ	0.5295	1LRY	BB2	0.9257	4QN6	LNV	0.4378
3H73	DNA	0.5718	1Q1Y	BB2	2.3749	5KV9	I57	1.1471
3TI3	LNV	0.4328	1SSZ	BB2	1.2646	1INH	ST6	0.8687
3TI6	G39	0.3460	2OS3	BB2	0.8713	1I7F	BCZ	0.3540
3TI8	LNV	0.4535	3E3U	NVC	0.7303	1I7G	BCZ	0.4746
4JE7	BB2	0.8267	4E9A	QAP	0.5152	5T8Z	BB2	0.7091
5I2B	BB2	0.7713	3CL0	G39	0.3994	2HT7	G39	0.5128

Table 2. The Interaction energy (kj/mol) of AChE and studied inhibitors obtained by molecular docking

Ligand code	ΔG (kj/mol)	Ligand code	ΔG (kj/mol)	Ligand code	ΔG (kj/mol)	Ligand code	ΔG (kj/mol)
4VV	-15.8172	GB	-12.0604	B3W	-17.4707	P6G	-10.9246
5GB	-13.6516	GL8	-13.8893	B3V	-23.5786	SCK	-12.2243
5GZ	-24.95	GMN	-15.4150	AA7	-3.1715	VXA	-12.0419
ZN4	-20.7391	GNT	-15.6246	A36	-23.1579	SO4	-11.6581
TZ5	-10.5999	HUX	-13.8401	ATJ	-13.1162	AE4	-8.9338
TNH	-21.7430	I40	-18.5550	ETM	-7.9629	1PE	-11.7707
TJH	-30.7445	NAF	-16.1984	HLO	-34.7418	DEP	-14.0186
SOF	-24.0018	NDG	-20.7377	MF2	-12.6524	VX	-15.0290
Q4Q	-21.5731	NWA	-10.2082	NTJ	-14.2055	EFS	-12.8749
PE4	-12.0153	PRM	-9.1282	OBI	-25.9574	5G8	-13.6516
P15	-9.3975	SAF	-19.0554	PGE	-11.3268	G6X	-10.9728
HUW	-16.1830	SCU	-11.1420	TFL	-23.8970	G3X	-11.8505
HUP	-14.6125	THA	-15.2270	FP1	-19.4458	AFT	-22.8637
HTB	-7.1524	K27	-22.1019	GC8	-19.7172	FP1	-17.4727
HI6	-28.3230	ACH	-11.9886	NHG	-19.8947	BMA	-14.4306
HBP	-20.0967	AT3	-9.8184	PZ5	-15.0158	CHT	-8.5180
EFS	-12.8749	X13	-1.4202	Z5K	-13.9569	DCU	-21.2847
E20	-27.5948	DME	-4.6489	A1E	-6.4493	E10	-11.0574
C57	-26.4061	H34	-11.8740	A2E	-4.6047	EDR	-15.4352
C56	-31.7773	NO3	-9.5901	A8B	-11.7649	FBQ	-20.3385
B3Z	-19.4197	NAG	-18.5179	A8N	-11.8723	FUL	-16.2992

Table 3. FlexX score of HLO derivatives in AChE active site

ZINC ID	ΔG (kj/mol)	ZINC ID	ΔG (kj/mol)	ZINC ID	ΔG (kj/mol)
ZINC00005077	-27.3784	ZINC68758087	-21.4063	ZINC68758091	-15.5140
ZINC05033416	-22.2578	ZINC04577910	-16.5619	ZINC92984347	-17.4974
ZINC01863576	-22.6564	ZINC15007645	-24.3008	ZINC92984332	-21.3727
ZINC19913394	-27.1784	ZINC18056228	-20.7744	ZINC78990672	-28.0314
ZINC05018113	-25.4189	ZINC70603710	-24.1592	ZINC79040001	-23.7272
ZINC01846393	-26.4366	ZINC33288079	-31.6016	ZINC68758496	-22.4302
ZINC95115865	-22.7513	ZINC78990209	-27.1988	ZINC15007565	-24.7233
ZINC05171075	-22.5787	ZINC78990204	-28.0080	ZINC70603431	-25.3969
ZINC20293508	-20.3434	ZINC68758023	-19.0376	ZINC82668666	-20.5966
ZINC20293511	-19.7444	ZINC68757301	-18.1518	ZINC70604507	-24.1599
ZINC01895559	-24.2650	ZINC82668669	-19.1049	ZINC70605318	-24.2189
ZINC00307025	-26.4089	ZINC82668692	-22 .4096	ZINC78986989	-24.7547
ZINC11681703	-23.7689	ZINC82668695	-20.2353	ZINC68759091	-23.3560
ZINC01777522	-24.6313	ZINC00123616	-35.4759	ZINC78956342	-22.1763
ZINC91363880	-24.3836	ZINC28861846	-26.9394	ZINC78988308	-23.9199
ZINC00174403	-29.0414	ZINC90349179	-21.6062	ZINC87753414	-22.5928
ZINC13126573	-30.1319	ZINC05421373	-17.3247	ZINC87028628	-26.9838
ZINC78954474	-35.4099	ZINC68759026	-24.3144	ZINC78987388	-31.1159
ZINC68757759	-16.9849	ZINC68758488	-20.8566	ZINC78995801	-26.2334
ZINC68757566	-18.9321	ZINC68758483	-22.7008	ZINC78989001	-29.5646
ZINC82668672	-20.5304	ZINC78948412	-23.7081	ZINC68756848	-20.7484
ZINC00520350	-20.3053	ZINC78949582	-29.5121	ZINC79003564	-25.4209
ZINC68757623	-16.2203	ZINC68758180	-16.5002	ZINC68758213	-21.3615
ZINC68758073	-16.5997	ZINC01791555	-21.9668	ZINC68758208	-16.3030
ZINC68757928	-18.8490	ZINC68757981	-15.2485	ZINC68757977	-20.7600
ZINC70603412	-25.1510	ZINC78990041	-25.7528	ZINC68757973	-21.9547
ZINC70605338	-28.5457	ZINC68757614	-23.1438	ZINC79041148	-27.6648
ZINC70604548	-26.6129	ZINC78997231	-23.3699	ZINC68758131	-17.1508
ZINC68757943	-20.0104	ZINC68758049	-18.5937	ZINC68758128	-15.9025
ZINC68757766	-21.9830	ZINC95221258	-22.3941	ZINC79038379	-30.3929
ZINC68758423	-20.2543	ZINC72226005	-20.6572	ZINC79038382	-27.7927
ZINC68758424	-21.2133	ZINC84846983	-24.3246	ZINC79041146	-30.2255
ZINC01851448	-24.2399	ZINC78988661	-22.6683	ZINC68756925	-22.8423
ZINC00436480	-34,5971	ZINC78988670	-24.6570	ZINC68756887	-22.4208
ZINC70605287	-27.2475	ZINC90283585	-26.6404	ZINC68756891	-21.2897
ZINC70605288	-29.0262	ZINC90283584	-29.0710	ZINC68756895	-21.4838
ZINC68757720	-22.2259	ZINC68757472	-20.7773	ZINC68756920	-23.7749
ZINC79041832	-25.5717	ZINC05119145	-24.2329	ZINC79007147	-25.1192
ZINC79041837	-25.4007	ZINC68758621	-17.5570	ZINC82668669	-19.1049
ZINC68758082	-21.1319	ZINC68758076	-17.2070		

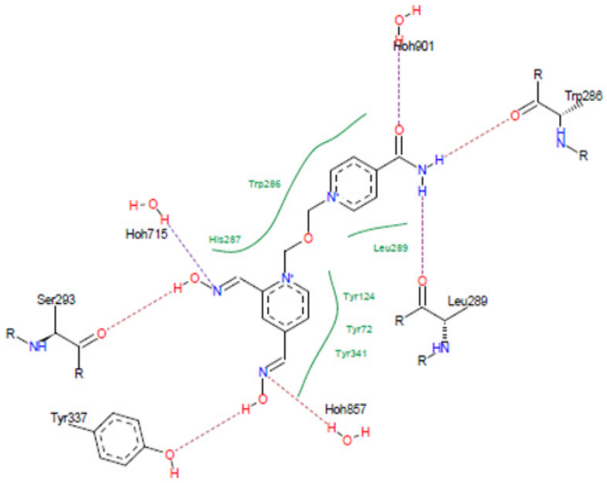

Figure 2. The docked poses of compound HLO within the binding pocket of AChE showing their different interactions (hydrogen bonds are shown in dotted lines and hydrophobic interactions are shown in green lines)

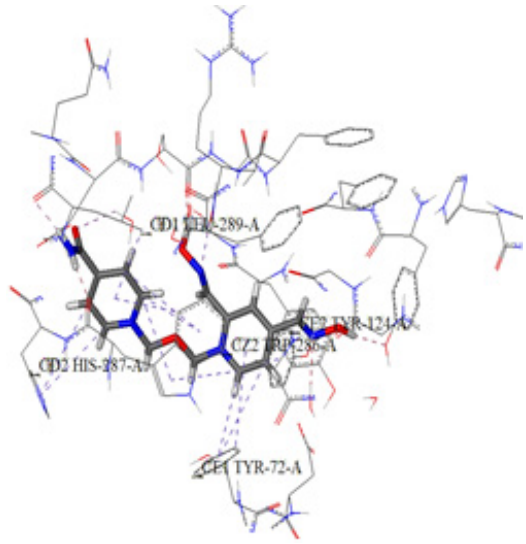

Figure 3. Representation of hydrophobic interactions formed by the inhibitor HLO

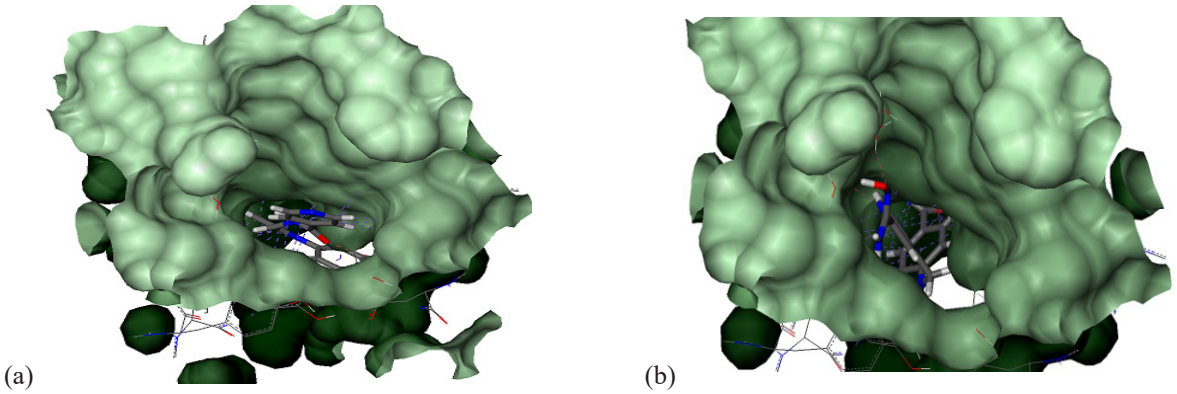

Figure 4. Illustration of the positioning of compounds ZINC00123616 (a) and ZINC78954474 (b) in the binding site of AchE

Three hydrophobic pockets stabilize the compound ZINC78954474 in the active site of AchE. Moreover, hydrophobic interactions are carried out with residues Gly121, Gly122, Tyr124, Trp286, Phe297, Tyr337, Phe338, Tyr341 and His447. In addition, the compound ZINC78954474 forms three hydrogen bonds with the binding site of AChE.

Previous studies explained the importance of the catalytic triad residues Ser203, Glu334 and His447 in the AChE active site [13] and also described the involvement of Tyr72, Tyr124 and Trp286 in the ligand binding in the peripheral site [14]. That Tyr72, Tyr124, Trp286 and His447 residues lying within the active site of the AChE, showed interactions with the compound ZINC78954474 suggest the possibility of applying this product for blocking the amino acids form interacting with the AChE for the degradation of acetylcholine.

The docking study showed that compounds ZINC00123616 (a) and ZINC78954474 (b) fit well into the binding site of AChE (Fig. 4). The FlexX software also helped to view the number and type of interactions involved in the ZINC00123616-AchE and ZINC78954474-AchE interactions.

Interestingly, the present study revealed that the hydrogen bonding of ZINC78954474 with Ser293 and Tyr337 is similar to that of the binding orientation of HLO in the AChE. This effect suggests that it can have a similar anti-Alzheimer propriety to HLO.

In addition, compounds ZINC00123616 and ZINC78954474 showed deep links within the AChE binding pocket through their pyridine and phenyl rings. These interact by hydrophobic means with Tyr341, Tyr124, Trp286, Gly122, Gly121, Phe297, Tyr337 and Phe338.

DihydrotanshinoneI was previously reported as a potent inhibitor of human AChE. In a study with AchE target protein, this compound, however, showed selective bonding to only the peripheral site [21], where it interacts with Trp286, Tyr337, Phe338, Phe297 and Tyr341 residues. In addition, Dihydrofuran was found to form a hydrogen bridge with Tyr124 hydroxyl [18]. As ZINC00123616, also demonstrated hydrogen-bonding interactions with Tyr124 and there are no direct links between them and amino acids of the catalytic pocket except with the His447 (Fig. 5), it could be concluded that it might also behave like Dihydrotanshinone I.

Territrem B is a high affinity inhibitor of AChE, and forms numerous hydrophobic interactions with the active site residues. These include contacts between the inhibitor and the residue Trp86 and His447 in the catalytic pocket, the side chain of Tyr337 at the interface between the catalytic and peripheral pockets, and interactions involving the side

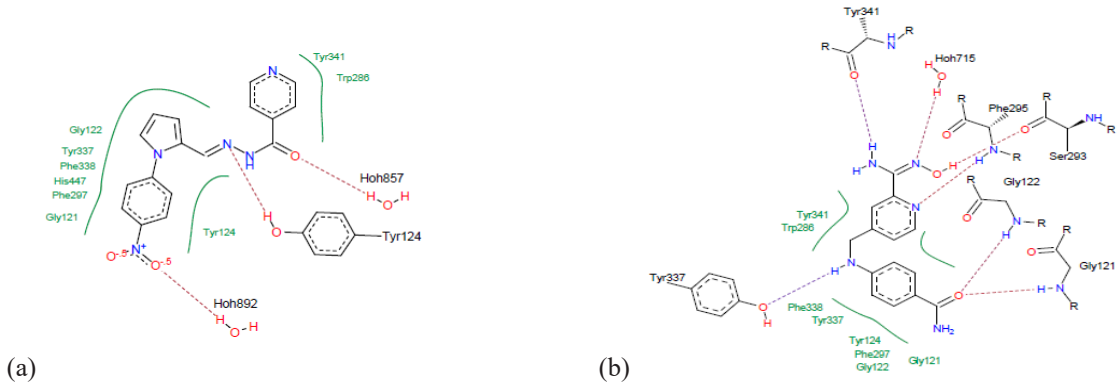

Figure 5. Interactions between ZINC00123616 (a), ZINC78954474 (b) and receptor protein residues (residue names indicated)

chains of Phe297, Tyr341and Phe338 with the inhibitor in the peripheral site [18]. These similarities in interaction of Territrem B to both the catalytic and peripheral pockets with the present studied compound, ZINC78954474, indicate that this compound is able to occupy the active site of human AChE and, hence, is involved in the inhibition of the enzyme.

Drug-likeness Prediction

In the subsequent part of our work, we verified the pharmacokinetic and toxicity proprieties of the most promising products (compounds ZINC78954474 and ZINC00123616) using Suissadme and PreADMET (Tab. 4). These properties consist of their blood-brain barrier (BBB) penetration, gastrointestinal absorption (GI), Cytochrome P450 (CYP) inhibition, Lipinski's rule of 5 catagorization, cell permeability (COCA-2) and toxicity. The same parameters of HLO were also studied for comparison.

Table 4. The predicted pharmacokinetic and toxicity proprieties of the most promising compounds

Properties	HLO	ZINC78954474	ZINC00123616
BBB permeant	0.0354779	0.0311664	0.304295
GI absorption	Hight	Hight	Hight
CYP inhibitor	CYP_2C9_inhibition CYP_2D6_inhibition	No	CYP2C19 inhibitor, CYP2C9 inhibitor
COCA-2[a]	21.0771	16.9076	6.20373
Lipinski's rule of 5	Suitable	Suitable	Suitable
Toxicity	hERG[b] inhibition (medium risk)	hERG inhibition (medium risk)	CR[c] hERG inhibition (medium risk)

[a] COCA-2: human colorectal carcinoma 2 cell permeability (nm/sec)
[b] hERG inhibition: human ether-ago- go related gene channel inhibition
[c] CR: carcinogenicity in rat

As indicated in Table 4, compound ZINC00123616 is predicted to have higher BBB penetration than that of HLO. Moreover, the studied products have high COCA-2 cell permeability, which insures their *in vivo* usage. Furthermore, compound ZINC78954474 does not inhibit CYP (essential enzymes for the metabolism of numerous medicaments in the liver) contrary to HLO, which inhibits CYP2D6 and CYP2D9. With no Lipinski's rule of 5 violation, both ZINC78954474 and ZINC00123616 follow the criteria for orally available drugs. Moreover, their toxicity problems (including CR and hERG inhibition for ZINC00123616 and hERG for ZINC78954474) can be improved during their further optimization to obtain clinically useful anti-Alzheimer's disease drugs.

CONCLUSION

In the present study, the molecular docking approch using FlexX was used to predict the binding energies and the interaction modes of 82 inhibitors derived from the Protein Data Bank and from a similar collection of HLO inhibitors from ZINC database for the AChE. Before performing the molecular docking, the docking protocol was validated by applying the RMSD test. This approach allowed us to suggest products ZINC00123616 and ZINC78954474 as potential new inhibitors of AChE. These proposed compounds were predicted to have good ADME/Tox properties.

CONFLICT OF INTEREST

The authors confirm that this article content has no conflicts of interest.

ACKNOWLEDGEMENTS

We are grateful to the Directorate General of Scientific Research and Technological Development, Algeria, for their support.

ORCID iDs

Merzoug Amina https://orcid.org/0000-0003-2280-757X

REFERNCES

1. Atlee JL. *Complications in Aanesthesia*. Philadelphia: Saunders Elsevier; 2007.
2. Burns A, Iliffe S. Alzheimer's disease. *BMJ.* 2009;338:b158.
3. Perry EK, Tomlinson BE, Blessed G, Bergmann K, Gibson PH, Perry RH. Correlation of cholinergic abnormalities with senile plaques and mental test scores in senile dementia. *Br Med J.* 1978;2(6150):1457-9.
4. Perry EK, Walker M, Grace J, Perry RH. Acetylcholine in mind: a neurotransmitter correlate of consciousness? *Trends Neurosci.* 1999; 22(6):273-80.
5. Draczkowski P, Tomaszuk A, Halczuk P, Strzemski M, Matosiuk D, Jozwiak K. Determination of affinity and efficacy of acetylcholinesterase inhibitors using isothermal titration calorimetry. *Biochim Biophys Acta Gen Subj.* 2016;1860(5):967-74.
6. Dhanjal JK, Sharma S, Grover A, Das A. Use of ligand-based pharmacophore modeling and docking approach to find novel acetylcholinesterase inhibitors for treating Alzheimer's. *Biomed Pharmacother.* 2015;71:146-52.

7. Chigurupati S, Selvaraj M, Mani V, Selvarajan KK, Mohammad JI, Kaveti B, et al. Identification of novel acetylcholinesterase inhibitors: indolopyrazoline derivatives and molecular docking studies. *Bioorg Chem*. 2016;67:9-17.
8. Lane RM, Kivipelto M, Greig NH. Acetylcholinesterase and its inhibition in Alzheimer disease. *Clin Neuropharmacol*. 2004;27:141-9.
9. Galisteo M, Rissel M, Sergent O, Chevanne M, Cillard J, Guillouzo A, et al. Hepatotoxicity of tacrine: occurrence of membrane fluidity alterations without involvement of lipid peroxidation. *J Pharmacol Exp Ther*. 2000;294:160-7.
10. Birks J. Cholinesterase inhibitors for Alzheimer's disease. *Cochrane Db Syst Rev*. 2006;1:CD005593.
11. Alldredge KB. *Applied therapeutics: The clinical use of drugs*. 10th ed. Baltimore: Wolters Kluwer Health/Lippincott Williams & Wilkins; 2013.
12. Chitranshi N, Gupta S, Tripathi PK, Seth PK. New molecular scaffolds for the design of Alzheimer's acetylcholinesterase inhibitors identified using ligand- and receptor-based virtual screening. *Med Chem Res*. 2013;2:2328-45.
13. Quinn DM. Acetylcholinesterase: Enzyme structure, reaction dynamics, and virtual transition states. *Chem Rev*. 1987;87:955-75.
14. Szegletes T, Mallender WD, Thomas PJ, Rosenberry TL. Substrate binding to the peripheral site of acetylcholinesterase initiates enzymatic catalysis. Substrate inhibition arises as a secondary effect. *Biochemistry*. 1999;38:122-33.
15. Bourne Y, Taylor P, Radic Z, Marchot P. Structural insights into ligand interactions at the acetylcholinesterase peripheral anionic site, *EMBO J*. 2003;22:1-12.
16. Dvir H, Silman I, Harel M, Rosenberry TL, Sussman JL. Acetylcholinesterase: From 3D structure to function. *Chem Biol Interact*. 2010;187:10-22.
17. Stahura FL, Bajorath J. Virtual screening methods that complement HTS. *Comb Chem High Throughput Screen*. 2004 ;7:259-69.
18. Cheung J, Gary EN, Shiomi K, Rosenberry TL. Structures of human acetylcholinesterase bound to dihydrotanshinone I and territrem B show peripheral site flexibility. *ACS Med Chem Lett*. 2013;11:1091-6.
19. Lipinski CA, Lombardo F, Dominy BW, Feeney PJ. Experimental and computational approaches to estimate solubility and permeability in drug discovery and development settings. *Adv Drug Deliv Rev*. 2001:46:3-26.
20. Grosdidier A. *Conception d'un logiciel de docking et applications dans la recherche de nouvelles molécules actives*. PhD Thesis : Joseph Fourier University, France; 2007.
21. Beri V, Wildman SA, Shiomi K, Al-Rashid Z, Cheung J, Rosenberry TL. The natural product dihydrotanshinone I provides a prototype for uncharged inhibitors that bind specifically to the acetylcholinesterase peripheral site with nanomolar affinity. *Biochem*. 2013; 52: 7486-99.